First Measurement of the Ratio $B(t \to Wb)/B(t \to Wq)$ and Associated Limit on the Cabibbo-Kobayashi-Maskawa Element $|V_{tb}|$

T. Affolder,[23] H. Akimoto,[45] A. Akopian,[38] M. G. Albrow,[11] P. Amaral,[8] S. R. Amendolia,[34] D. Amidei,[26] K. Anikeev,[24] J. Antos,[1] G. Apollinari,[11] T. Arisawa,[45] T. Asakawa,[43] W. Ashmanskas,[8] F. Azfar,[31] P. Azzi-Bacchetta,[32] N. Bacchetta,[32] M. W. Bailey,[28] S. Bailey,[16] P. de Barbaro,[37] A. Barbaro-Galtieri,[23] V. E. Barnes,[36] B. A. Barnett,[19] S. Baroiant,[5] M. Barone,[13] G. Bauer,[24] F. Bedeschi,[34] S. Belforte,[42] W. H. Bell,[15] G. Bellettini,[34] J. Bellinger,[46] D. Benjamin,[10] J. Bensinger,[4] A. Beretvas,[11] J. P. Berge,[11] J. Berryhill,[8] B. Bevensee,[33] A. Bhatti,[38] M. Binkley,[11] D. Bisello,[32] M. Bishai,[11] R. E. Blair,[2] C. Blocker,[4] K. Bloom,[26] B. Blumenfeld,[19] S. R. Blusk,[37] A. Bocci,[38] A. Bodek,[37] W. Bokhari,[33] G. Bolla,[36] Y. Bonushkin,[6] D. Bortoletto,[36] J. Boudreau,[35] A. Brandl,[28] S. van den Brink,[19] C. Bromberg,[27] M. Brozovic,[10] N. Bruner,[28] E. Buckley-Geer,[11] J. Budagov,[9] H. S. Budd,[37] K. Burkett,[16] G. Busetto,[32] A. Byon-Wagner,[11] K. L. Byrum,[2] P. Calafiura,[23] M. Campbell,[26] W. Carithers,[23] J. Carlson,[26] D. Carlsmith,[46] W. Caskey,[5] J. Cassada,[37] A. Castro,[32] D. Cauz,[42] A. Cerri,[34] A. W. Chan,[1] P. S. Chang,[1] P. T. Chang,[1] J. Chapman,[26] C. Chen,[33] Y. C. Chen,[1] M.-T. Cheng,[1] M. Chertok,[40] G. Chiarelli,[34] I. Chirikov-Zorin,[9] G. Chlachidze,[9] F. Chlebana,[11] L. Christofek,[18] M. L. Chu,[1] Y. S. Chung,[37] C. I. Ciobanu,[29] A. G. Clark,[14] A. Connolly,[23] J. Conway,[39] M. Cordelli,[13] J. Cranshaw,[41] D. Cronin-Hennessy,[10] R. Cropp,[25] R. Culbertson,[11] D. Dagenhart,[44] S. D'Auria,[15] F. DeJongh,[11] S. Dell'Agnello,[13] M. Dell'Orso,[34] L. Demortier,[38] M. Deninno,[3] P. F. Derwent,[11] T. Devlin,[39] J. R. Dittmann,[11] S. Donati,[34] J. Done,[40] T. Dorigo,[16] N. Eddy,[18] K. Einsweiler,[23] J. E. Elias,[11] E. Engels, Jr.,[35] R. Erbacher,[11] D. Errede,[18] S. Errede,[18] Q. Fan,[37] R. G. Feild,[47] J. P. Fernandez,[11] C. Ferretti,[34] R. D. Field,[12] I. Fiori,[3] B. Flaugher,[11] G. W. Foster,[11] M. Franklin,[16] J. Freeman,[11] J. Friedman,[24] Y. Fukui,[22] I. Furic,[24] S. Galeotti,[34] M. Gallinaro,[38] T. Gao,[33] M. Garcia-Sciveres,[23] A. F. Garfinkel,[36] P. Gatti,[32] C. Gay,[47] D. W. Gerdes,[26] P. Giannetti,[34] P. Giromini,[13] V. Glagolev,[9] D. Glenzinski,[11] M. Gold,[28] J. Goldstein,[11] A. Gordon,[16] I. Gorelov,[28] A. T. Goshaw,[10] Y. Gotra,[35] K. Goulianos,[38] C. Green,[36] G. Grim,[5] P. Gris,[11] L. Groer,[39] C. Grosso-Pilcher,[8] M. Guenther,[36] G. Guillian,[26] J. Guimaraes da Costa,[16] R. M. Haas,[12] C. Haber,[23] E. Hafen,[24] S. R. Hahn,[11] C. Hall,[16] T. Handa,[17] R. Handler,[46] W. Hao,[41] F. Happacher,[13] K. Hara,[43] A. D. Hardman,[36] R. M. Harris,[11] F. Hartmann,[20] K. Hatakeyama,[38] J. Hauser,[6] J. Heinrich,[33] A. Heiss,[20] M. Herndon,[19] C. Hill,[5] K. D. Hoffman,[36] C. Holck,[33] R. Hollebeek,[33] L. Holloway,[18] R. Hughes,[29] J. Huston,[27] J. Huth,[16] H. Ikeda,[43] J. Incandela,[11] G. Introzzi,[34] J. Iwai,[45] Y. Iwata,[17] E. James,[26] H. Jensen,[11] M. Jones,[33] U. Joshi,[11] H. Kambara,[14] T. Kamon,[40] T. Kaneko,[43] K. Karr,[44] H. Kasha,[47] Y. Kato,[30] T. A. Keaffaber,[36] K. Kelley,[24] M. Kelly,[26] R. D. Kennedy,[11] R. Kephart,[11] D. Khazins,[10] T. Kikuchi,[43] B. Kilminster,[37] B. J. Kim,[21] D. H. Kim,[21] H. S. Kim,[18] M. J. Kim,[21] S. H. Kim,[43] Y. K. Kim,[23] M. Kirby,[10] M. Kirk,[4] L. Kirsch,[4] S. Klimenko,[12] P. Koehn,[29] A. Köngeter,[20] K. Kondo,[45] J. Konigsberg,[12] K. Kordas,[25] A. Korn,[24] A. Korytov,[12] E. Kovacs,[2] J. Kroll,[33] M. Kruse,[37] S. E. Kuhlmann,[2] K. Kurino,[17] T. Kuwabara,[43] A. T. Laasanen,[36] N. Lai,[8] S. Lami,[38] S. Lammel,[11] J. I. Lamoureux,[4] J. Lancaster,[10] M. Lancaster,[23] R. Lander,[5] G. Latino,[34] T. LeCompte,[2] A. M. Lee IV,[10] K. Lee,[41] S. Leone,[34] J. D. Lewis,[11] M. Lindgren,[6] T. M. Liss,[18] J. B. Liu,[37] Y. C. Liu,[1] D. O. Litvintsev,[8] O. Lobban,[41] N. Lockyer,[33] J. Loken,[31] M. Loreti,[32] D. Lucchesi,[32] P. Lukens,[11] S. Lusin,[46] L. Lyons,[31] J. Lys,[23] R. Madrak,[16] K. Maeshima,[11] P. Maksimovic,[16] L. Malferrari,[3] M. Mangano,[34] M. Mariotti,[32] G. Martignon,[32] A. Martin,[47] J. A. J. Matthews,[28] J. Mayer,[25] P. Mazzanti,[3] K. S. McFarland,[37] P. McIntyre,[40] E. McKigney,[33] M. Menguzzato,[32] A. Menzione,[34] C. Mesropian,[38] A. Meyer,[11] T. Miao,[11] R. Miller,[27] J. S. Miller,[26] H. Minato,[43] S. Miscetti,[13] M. Mishina,[22] G. Mitselmakher,[12] N. Moggi,[3] E. Moore,[28] R. Moore,[26] Y. Morita,[22] T. Moulik,[24] M. Mulhearn,[24] A. Mukherjee,[11] T. Muller,[20] A. Munar,[34] P. Murat,[11] S. Murgia,[27] J. Nachtman,[6] V. Nagaslaev,[41] S. Nahn,[47] H. Nakada,[43] T. Nakaya,[8] I. Nakano,[17] C. Nelson,[11] T. Nelson,[11] C. Neu,[29] D. Neuberger,[20] C. Newman-Holmes,[11] C.-Y. P. Ngan,[24] H. Niu,[4] L. Nodulman,[2] A. Nomerotski,[12] S. H. Oh,[10] T. Ohmoto,[17] T. Ohsugi,[17] R. Oishi,[43] T. Okusawa,[30] J. Olsen,[46] W. Orejudos,[23] C. Pagliarone,[34] F. Palmonari,[34] R. Paoletti,[34] V. Papadimitriou,[41] S. P. Pappas,[47] D. Partos,[4] J. Patrick,[11] G. Pauletta,[42] M. Paulini,[23,*] C. Paus,[24] L. Pescara,[32] T. J. Phillips,[10] G. Piacentino,[34] K. T. Pitts,[18] A. Pompos,[36] L. Pondrom,[46] G. Pope,[35] M. Popovic,[25] F. Prokoshin,[9] J. Proudfoot,[2] F. Ptohos,[13] O. Pukhov,[9] G. Punzi,[34] K. Ragan,[25] A. Rakitine,[24] D. Reher,[23] A. Reichold,[31] A. Ribon,[32] W. Riegler,[16] F. Rimondi,[3] L. Ristori,[34] M. Riveline,[25] W. J. Robertson,[10] A. Robinson,[25] T. Rodrigo,[7] S. Rolli,[44] L. Rosenson,[24] R. Roser,[11] R. Rossin,[32] A. Roy,[24] A. Safonov,[38] R. St. Denis,[15] W. K. Sakumoto,[37] D. Saltzberg,[6] C. Sanchez,[29] A. Sansoni,[13] L. Santi,[42] H. Sato,[43] P. Savard,[25] P. Schlabach,[11] E. E. Schmidt,[11] M. P. Schmidt,[47] M. Schmitt,[16] L. Scodellaro,[32] A. Scott,[6] A. Scribano,[34] S. Segler,[11] S. Seidel,[28] Y. Seiya,[43] A. Semenov,[9] F. Semeria,[3] T. Shah,[24] M. D. Shapiro,[23] P. F. Shepard,[35]

0031-9007/01/86(15)/3233(6)$15.00 © 2001 The American Physical Society

T. Shibayama,[43] M. Shimojima,[43] M. Shochet,[8] J. Siegrist,[23] A. Sill,[41] P. Sinervo,[25] P. Singh,[18] A.J. Slaughter,[47] K. Sliwa,[44] C. Smith,[19] F.D. Snider,[11] A. Solodsky,[38] J. Spalding,[11] T. Speer,[14] P. Sphicas,[24] F. Spinella,[34] M. Spiropulu,[16] L. Spiegel,[11] J. Steele,[46] A. Stefanini,[34] J. Strologas,[18] F. Strumia,[14] D. Stuart,[11] K. Sumorok,[24] T. Suzuki,[43] T. Takano,[30] R. Takashima,[17] K. Takikawa,[43] P. Tamburello,[10] G.F. Tartarelli,[34] M. Tanaka,[43] B. Tannenbaum,[6] W. Taylor,[25] M. Tecchio,[26] R. Tesarek,[11] P.K. Teng,[1] K. Terashi,[38] S. Tether,[24] A.S. Thompson,[15] R. Thurman-Keup,[2] P. Tipton,[37] S. Tkaczyk,[11] K. Tollefson,[37] A. Tollestrup,[11] H. Toyoda,[30] W. Trischuk,[25] J.F. de Troconiz,[16] J. Tseng,[24] N. Turini,[34] F. Ukegawa,[43] T. Vaiciulis,[37] J. Valls,[39] S. Vejcik III,[11] G. Velev,[11] R. Vidal,[11] R. Vilar,[7] I. Volobouev,[23] D. Vucinic,[24] R.G. Wagner,[2] R.L. Wagner,[11] J. Wahl,[8] N.B. Wallace,[39] A.M. Walsh,[39] C. Wang,[10] M.J. Wang,[1] T. Watanabe,[43] D. Waters,[31] T. Watts,[39] R. Webb,[40] H. Wenzel,[20] W.C. Wester III,[11] A.B. Wicklund,[2] E. Wicklund,[11] T. Wilkes,[5] H.H. Williams,[33] P. Wilson,[11] B.L. Winer,[29] D. Winn,[26] S. Wolbers,[11] D. Wolinski,[26] J. Wolinski,[27] S. Wolinski,[26] S. Worm,[28] X. Wu,[14] J. Wyss,[34] A. Yagil,[11] W. Yao,[23] G.P. Yeh,[11] P. Yeh,[1] J. Yoh,[11] C. Yosef,[27] T. Yoshida,[30] I. Yu,[21] S. Yu,[33] Z. Yu,[47] A. Zanetti,[42] F. Zetti,[23] and S. Zucchelli[3]

(CDF Collaboration)

[1]*Institute of Physics, Academia Sinica, Taipei, Taiwan 11529, Republic of China*
[2]*Argonne National Laboratory, Argonne, Illinois 60439*
[3]*Istituto Nazionale di Fisica Nucleare, University of Bologna, I-40127 Bologna, Italy*
[4]*Brandeis University, Waltham, Massachusetts 02254*
[5]*University of California at Davis, Davis, California 95616*
[6]*University of California at Los Angeles, Los Angeles, California 90024*
[7]*Instituto de Fisica de Cantabria, CSIC-University of Cantabria, 39005 Santander, Spain*
[8]*Enrico Fermi Institute, University of Chicago, Chicago, Illinois 60637*
[9]*Joint Institute for Nuclear Research, RU-141980 Dubna, Russia*
[10]*Duke University, Durham, North Carolina 27708*
[11]*Fermi National Accelerator Laboratory, Batavia, Illinois 60510*
[12]*University of Florida, Gainesville, Florida 32611*
[13]*Laboratori Nazionali di Frascati, Istituto Nazionale di Fisica Nucleare, I-00044 Frascati, Italy*
[14]*University of Geneva, CH-1211 Geneva 4, Switzerland*
[15] *Glasgow University, Glasgow G12 8QQ, United Kingdom*
[16]*Harvard University, Cambridge, Massachusetts 02138*
[17]*Hiroshima University, Higashi-Hiroshima, 724 Japan*
[18]*University of Illinois, Urbana, Illinois 61801*
[19]*The Johns Hopkins University, Baltimore, Maryland 21218*
[20]*Institut für Experimentelle Kernphysik, Universität Karlsruhe, 76128 Karlsruhe, Germany*
[21]*Center for High Energy Physics, Kyungpook National University, Taegu 702-701, Korea; Seoul National University, Seoul 151-742, Korea; and Sung Kyun Kwan University, Suwon 440-746 Korea*
[22]*High Energy Accelerator Research Organization (KEK), Tsukuba, Ibaraki 305, Japan*
[23]*Ernest Orlando Lawrence Berkeley National Laboratory, Berkeley, California 94720*
[24]*Massachusetts Institute of Technology, Cambridge, Massachusetts 02139*
[25]*Institute of Particle Physics, McGill University, Montreal H3A 2T8, Canada; and University of Toronto, Toronto M5S 1A7, Canada*
[26]*University of Michigan, Ann Arbor, Michigan 48109*
[27]*Michigan State University, East Lansing, Michigan 48824*
[28]*University of New Mexico, Albuquerque, New Mexico 87131*
[29]*The Ohio State University, Columbus, Ohio 43210*
[30]*Osaka City University, Osaka 588, Japan*
[31]*University of Oxford, Oxford OX1 3RH, United Kingdom*
[32]*Universita di Padova, Istituto Nazionale di Fisica Nucleare, Sezione di Padova, I-35131 Padova, Italy*
[33]*University of Pennsylvania, Philadelphia, Pennsylvania 19104*
[34]*Istituto Nazionale di Fisica Nucleare, University and Scuola Normale Superiore of Pisa, I-56100 Pisa, Italy*
[35]*University of Pittsburgh, Pittsburgh, Pennsylvania 15260*
[36]*Purdue University, West Lafayette, Indiana 47907*
[37]*University of Rochester, Rochester, New York 14627*
[38]*Rockefeller University, New York, New York 10021*
[39]*Rutgers University, Piscataway, New Jersey 08855*
[40]*Texas A&M University, College Station, Texas 77843*

[41]Texas Tech University, Lubbock, Texas 79409
[42]Istituto Nazionale di Fisica Nucleare, University of Trieste, Udine, Italy
[43]University of Tsukuba, Tsukuba, Ibaraki 305, Japan
[44]Tufts University, Medford, Massachusetts 02155
[45]Waseda University, Tokyo 169, Japan
[46]University of Wisconsin, Madison, Wisconsin 53706
[47]Yale University, New Haven, Connecticut 06520
(Received 7 December 2000)

We present the first measurement of the ratio of branching fractions $R \equiv B(t \rightarrow Wb)/B(t \rightarrow Wq)$ from $p\bar{p}$ collisions at $\sqrt{s} = 1.8$ TeV. The data set corresponds to 109 pb^{-1} of data recorded by the Collider Detector at Fermilab during the 1992–95 Tevatron run. We measure $R = 0.94^{+0.31}_{-0.24}(\text{stat} + \text{syst})$ or $R > 0.61$ (0.56) at 90% (95)% C.L., in agreement with the standard model predictions. This measurement yields a limit on the Cabibbo-Kobayashi-Maskawa quark mixing matrix element $|V_{tb}|$ under the assumption of three generations and unitarity.

DOI: 10.1103/PhysRevLett.86.3233 PACS numbers: 12.15.Hh, 13.85.Ni, 14.65.Ha

The Cabibbo-Kobayashi-Maskawa matrix [1] is a fundamental component of the standard model of electroweak interactions. However, the matrix elements must be determined experimentally since the model does not constrain their values. Some of the matrix elements have been determined by studying the weak decay of quarks or by deep inelastic neutrino scattering experiments. Until now no direct information has been available for the elements of the top sector. The matrix elements $|V_{td}|$ and $|V_{ts}|$ have been indirectly estimated using measurements of processes that probe loop diagrams involving the top quark. Using these indirect measurements and a global fit which includes the additional assumptions of three generations and unitarity the allowed range of $|V_{tb}|$ is 0.9989–0.9993 (at 90% C.L.) [2]. The large value of $|V_{tb}|$ implies that R, the ratio of branching fractions $B(t \rightarrow Wb)/B(t \rightarrow Wq)$ (where q is a d, s, or b quark), is close to unity and that the branching ratio for the decay of a top quark to Wb is nearly 100%. The identification of $t\bar{t}$ events at the Tevatron allows us to directly check for a possible deviation from the range found by the global fits which would imply the appearance of new physics. The prediction of R being close to unity has been used in the discovery of the top quark and in the measurement of its cross section but has not been, until now, confirmed experimentally.

In this Letter we present the first direct measurement of R. The result provides additional support for the top quark discovery. Under the assumption of unitarity and three generations, it also provides a constraint on the CKM element $|V_{tb}|$ obtained by direct measurement in top events. The analysis is performed using 109 pb^{-1} of proton-antiproton collisions data recorded at a center of mass energy of 1.8 TeV by the Collider Detector at Fermilab (CDF) during the 1992–1995 run of the Tevatron Collider at Fermilab. The CDF detector is described in detail elsewhere [3]; here we briefly describe only the components which play a major role in this analysis.

The CDF tracking system consists of three different detectors embedded in a 1.4 T solenoidal magnetic field. A particle emerging from the interaction region passes through a four-layer silicon vertex detector (SVX) [4,5] located just outside the beam pipe, a set of vertex time projection chambers (VTX), and a drift chamber (CTC) with 84 measuring planes. The CTC performs the pattern recognition and a three-dimensional reconstruction of charged particles. The VTX measures the position of the primary interaction vertex along the beam axis. Finally, the SVX, with its $r - \varphi$ readout in the plane perpendicular to the colliding beams, is designed to determine precisely the impact parameter of the tracks. A momentum resolution of $\Delta P_T/P_T^2 \simeq 0.0009\ (\text{GeV}/c)^{-1}$ [6] and an asymptotic impact parameter resolution of $\simeq$13 μm is obtained for tracks with high P_T detected by the SVX and the CTC. Outside the tracking volume, electromagnetic and hadronic calorimeters measure the energy of particles in the region $|\eta| \leq 4.2$ [7]. Electron identification is obtained by combining calorimetric and tracking information. Muon identification is performed by matching tracks reconstructed in the CTC with segments measured by a system of drift chambers (muon chambers) located outside the calorimeters and covering the region $|\eta| < 1$.

The top quark has been observed [8–10] only when produced in pairs. Assuming that the top quark decays to a real W boson, it is customary to classify $t\bar{t}$ final states according to the decay modes of the two W bosons. We use two $t\bar{t}$ candidate data sets: the lepton + jets (l + jets) and the dilepton samples. The l + jets sample, in which one W decays to an electron or a muon and its corresponding neutrino and the other W decays into two jets, has a final state characterized by a high-P_T lepton, missing transverse energy $\not{E}_T$ [11], and four jets. The dilepton sample, in which both W bosons decay into electrons or muons and neutrinos, is characterized by a final state with missing transverse energy, two high-P_T leptons, and two jets. The selection criteria required to identify the W bosons and to enhance the top quark content in these data sets have been described in detail in previous CDF publications [8,9]. To isolate the l + jets sample we require the presence of one central ($|\eta| < 1$) lepton (e or μ) with $P_T > 20$ GeV/c, $\not\!\!E_T > 20$ GeV, three jets with $E_T > 15$ [12] GeV within $|\eta| < 2$ and a fourth jet with $E_T > 8$ GeV within $|\eta| < 2.4$. In the dilepton sample we require two leptons (e or μ) with $P_T > 20$ GeV/c, $\not\!\!E_T > 25$ GeV and two jets with $E_T > 10$ GeV in the region $|\eta| < 2.0$. Candidate Z events are removed by rejecting events containing same-flavor lepton pairs with opposite charge whose invariant mass lies between 75 and 105 GeV/c^2. By construction the two data sets have no overlap. After applying all the selection criteria we find 163 events in the l + jets and 9 events in the dilepton sample.

The presence of the $t \to Wb$ decay is deduced by identifying jets associated with b hadron decays using two distinct algorithms: the SVX tagger and the SLT tagger. The SVX tagging algorithm [9] relies on the long lifetime of b hadrons. It searches for b hadron decay vertices which are significantly displaced from the primary vertex and have three or more associated tracks. If this search fails, tighter quality cuts are applied to the tracks within the jet and vertices with two tracks are also accepted. In both cases, the transverse displacement of the decay vertex from the primary vertex, divided by its uncertainty, is required to be larger than 3. The SVX algorithm is characterized by an efficiency (ε_s) to tag a single b jet in a $t\bar{t}$ event of (37.0 $\pm$ 3.7)% and by a fake tagging rate of about 0.5%. The SLT tagging is performed by looking for low-P_T (relatively soft compared to the primary lepton) muons and electrons from semileptonic b hadron decays. The algorithm looks for low transverse momentum electron and muon candidates by matching CTC tracks with $P_T > 2$ GeV/c with calorimeter clusters and track segments in the muon chambers. Moreover, to classify the event as a $t\bar{t}$ candidate, the soft lepton is required to be within a conus of radius 0.4 in the η-ϕ space from one of the four highest-E_T jets in the event. The SLT algorithm has an efficiency per jet (ε_l) of (10.2 $\pm$ 1.0)% and a fake tagging rate of about 2%. Efficiencies for the SLT and SVX algorithms are calculated using the low-P_T inclusive lepton sample enriched in $b\bar{b}$ production and Monte Carlo simulation. The background due to fake tags is measured for both algorithms using generic jet samples. A detailed discussion of the algorithms, the determination of the tagging efficiency, and the fake rate can be found in [13].

The unknown ratio of branching fractions, R, is measured by comparing the observed number of tags in the data with expectations based on selection criteria acceptances, tagging efficiencies, and background estimates. In the dilepton sample only SVX tagging is used and the sample is divided into three nonoverlapping bins: events with no b-tags (bin 0), one and only one b-tag (bin 1) and two b-tags (bin 2). The use of SLT tagging in the dilepton data set does not provide any additional statistical gain. In the l + jets sample, we use both the SVX and SLT algorithms. Monte Carlo studies [14] indicate that a superior use of the tagging information is obtained by dividing events into the same three bins used for the dilepton sample and then by subdividing the bin with no SVX tags into two bins according to the SLT tagging status. The first bin (bin 00) is populated by events which are tagged by neither the SVX nor the SLT algorithm and the second one (bin 01) contains events with one or more SLT tags and no SVX tags.

The number of observed events in each bin is reported in Table I. The expected number of events, N_i, in each of the bins of the l + jets sample can be expressed as a function of the acceptances, tagging efficiencies, and the estimated background by the following set of equations:

$$N_{00} = n_0 + (1 - \varepsilon_l)(1 - \varepsilon_s)n_1 + (1 - \varepsilon_l)^2(1 - \varepsilon_s)^2 n_2 + F_{00}\,, \tag{1a}$$

$$N_{01} = \varepsilon_l(1 - \varepsilon_s)n_1 + \varepsilon_l(2 - \varepsilon_l)(1 - \varepsilon_s)^2 n_2 + F_{01}\,, \tag{1b}$$

$$N_1 = \varepsilon_s n_1 + 2\varepsilon_s(1 - \varepsilon_s)n_2 + F_1\,, \tag{1c}$$

$$N_2 = \varepsilon_s^2 n_2 + F_2\,, \tag{1d}$$

with $n_i (i = 0, 1, 2)$, the number of events with i b-jets in the SVX acceptance, given by

$$n_0 = N_{\rm top}[a_0 + (1 - R)a_1 + (1 - R)^2 a_2]\,, \tag{2a}$$

$$n_1 = N_{\rm top}[Ra_1 + 2R(1 - R)a_2]\,, \tag{2b}$$

$$n_2 = N_{\rm top}R^2 a_2\,, \tag{2c}$$

where $N_{\rm top}$ is the total number of $t\bar{t}$ events in the sample, F_i is the background in the ith bin, and a_i is the fraction of events containing i b jets ($i = 0, 1, 2$) in the acceptance. This definition of acceptance, which reflects the way the a_i's are related to R in Eqs. (2a)–(2c), has been chosen in order to be able to use the standard CDF top Monte Carlo (see below) which assumes $R = 1$. For the dilepton sample, Eqs. (1a) and (1b) are merged into one because SLT tagging is not used.

The unknown ratio R is obtained by minimizing the negative logarithm of a likelihood function. Since the l + jets and dilepton samples are independent, the global likelihood can be written as

$$\mathcal{L} = \mathcal{L}_{\ell+\rm jets}\mathcal{L}_{\rm dilepton} \tag{3}$$

where each of the individual likelihoods is of the form

$$\mathcal{L}_\alpha = \prod_i P(N_i; \bar{N}_i) \prod_j G(x_j; \bar{x}_j, \sigma_j)\,.$$

TABLE I. Number of events for the two data samples in each of the bins defined according to the number of SVX and SLT tags. The case of SLT tags (bin 01 = "one or more SLT tag, no SVX tag") does not apply ("n/a") to the dilepton data set (see text).

Sample	00	01	1	2
l + jets	126	14	18	5
dilepton	6	n/a	3	0

TABLE II. Estimated number of background events bin by bin for the two data samples. The case of SLT tags (bin 01) applies only to the l + jets data set and the double tagged dilepton background is neglected ("n/a").

Sample	00	01	1	2
l + jets	108 ± 10	7.2 ± 1.6	$3.3^{+2.3}_{-1.2}$	0.2 ± 0.1
dilepton	2.3 ± 0.5	n/a	0.10 ± 0.04	n/a

In this expression, $P(N_i; \bar{N}_i)$ is the Poisson probability for observing N_i events in each bin (the index i runs from 1 to 4 for the l + jets sample and from 1 to 3 for the dilepton one) with an expected mean $\bar{N}_i$ (see Table I). The functions $G(x_j; \bar{x}_j, \sigma_j)$ are Gaussians in x_j, with mean $\bar{x}_j$ and variance σ_j^2, and incorporate the uncertainties in the tagging efficiencies, backgrounds, and acceptances into the likelihood functions.

The acceptances and efficiencies are obtained using a $t\bar{t}$ Monte Carlo ($M_{\text{top}} = 175\ \text{GeV}/c^2$) data set generated using PYTHIA [15], combined with a detailed simulation of the detector response. The total number of $t\bar{t}$ pairs (N_{top}) in the two data samples is left as a free parameter. The acceptances in each bin are normalized with respect to the bin with no b jets. As a consequence, the trigger and lepton identification efficiencies cancel out in the ratio. We obtain $r_1 = 11.8 \pm 1.2$ (14.5 ± 1.4) and $r_2 = 38.7 \pm 3.9$ (58.5 ± 5.8), where $r_i = a_i/a_0$, for the l + jets (dilepton) sample. The uncertainties in these ratios include contributions from the jet energy scale and from the Monte Carlo modeling of initial and final state radiation.

The background in the untagged sample is mainly due to the associated production of W bosons with light quark jets. The backgrounds to the SLT and SVX tagged events (background in bin 01 and 1, respectively), are mainly due to the associated production of W bosons and heavy quarks ($Wb\bar{b}$, $Wc\bar{c}$, Wc) and to mistags due to mismeasured tracks. Smaller contributions come from $b\bar{b}$, diboson production (WW, ZZ, and WZ), $Z \rightarrow \tau\tau$ decays, Drell-Yan lepton pair production and single top quark production. These backgrounds are calculated using a combination of data and Monte Carlo information [14,16]. The initial values of the SVX and SLT backgrounds are a function of the $t\bar{t}$ content of the l + jets sample itself, and therefore need to be appropriately corrected [8]. An iterative process is used to account for this effect and has been implemented in the likelihood minimization procedure used to estimate R. Using this procedure as output of the likelihood minimization, we estimate $F_1 = 3.3^{+2.3}_{-1.2}$ and $F_{01} = 7.2 \pm 1.6$ events for the SVX and SLT backgrounds, respectively. In the same way, the background to double SVX tagged events (bin 2) is estimated to be small and amounts to $F_2 = 0.2 \pm 0.1$ events. The background in bin 00, F_{00}, is obtained as follows. Defining N_{tot} to be the total number of events in the l + jets data set, N_{SVX} the total number of SVX tagged events in this sample, F_{SVX} the estimated background and ϵ_{SVX} the SVX event tagging efficiency, the total number of top events is $N_{t\bar{t}} = (N_{\text{SVX}} - F_{\text{SVX}})/(\epsilon_{\text{SVX}} R)$. The number of background events before tagging is given by $F = N_{\text{tot}} - N_{t\bar{t}}$ and therefore the background in bin 00 is $F_{00} = F - (F_{01} + F_1 + F_2)$. As before, the estimate is performed iteratively during the likelihood minimization.

The initial background to the dilepton sample has been estimated to be 2.4 ± 0.5 [17]. In this sample, we estimate a background of 0.10 ± 0.04 events to SVX single tagged events. The double SVX tagged background is negligible [$F_2 = 0$ in Eq. (1d)]. In this case, the number of background events is not a function of the $t\bar{t}$ content of the initial sample and no special correction needs to be applied. As in the l + jets case, the background in bin 0 is obtained by a subtraction of the tagged background from the total background and amounts to 2.3 ± 0.5 events. The resulting number of background events after the likelihood minimization procedure is shown in Table II for both data sets.

The likelihood minimization yields $R = 0.94^{+0.31}_{-0.24}$(stat + syst) or, splitting the statistical and

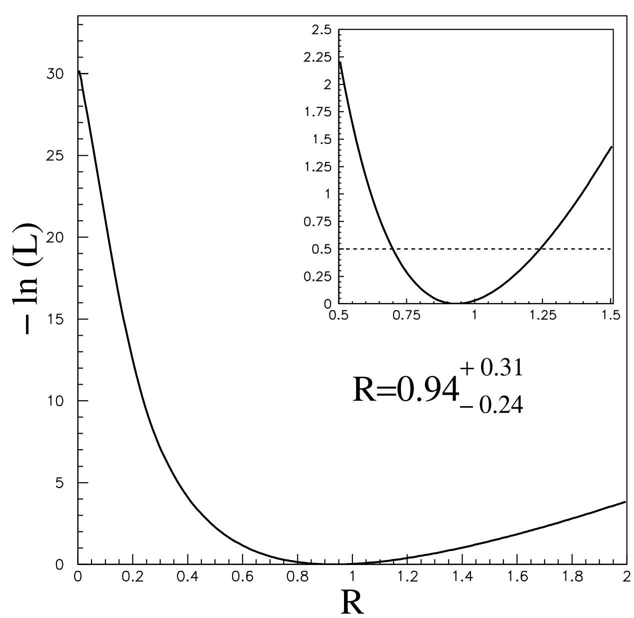

FIG. 1. The negative logarithm of the likelihood function of Eq. (3) as a function of R. The inset plot is a magnified view of the region around the minimum.

systematical uncertainties, $R = 0.94^{+0.26}_{-0.21}(\text{stat})^{+0.17}_{-0.12}(\text{syst})$. The negative log-likelihood as a function of R is shown in Fig. 1. The lower limit on R is obtained by a numerical integration of the likelihood function and we obtain $R > 0.61$ (0.56) at 90% (95)% C.L.

The CKM element $|V_{tb}|$ is directly related to R, although in a model-dependent way. We assume that the top quark decays to non-W final states are negligible [18,19]. Under this assumption R is related to $|V_{tb}|$ by

$$R = \frac{|V_{tb}|^2}{|V_{ts}|^2 + |V_{td}|^2 + |V_{tb}|^2}\,. \tag{4}$$

If we assume three generation unitarity, the denominator is equal to unity and therefore $R = |V_{tb}|^2$. As a consequence, we obtain $|V_{tb}| = 0.97^{+0.16}_{-0.12}$ or $|V_{tb}| > 0.78$ (0.75) at 90% (95)% C.L.

The result, although limited by statistics, represents the first direct measurement of R. The large value of R that we measure is consistent with standard model expectations and supports the assumption that top quarks decay predominantly to b quarks. Under the assumption of three generation unitarity, our calculated value of $|V_{tb}| = 0.97^{+0.16}_{-0.12}$ ($|V_{tb}| > 0.78$ at 90% C.L.) is consistent with indirect limits obtained from global fits.

We thank the Fermilab staff and the technical staffs of the participating institutions for their vital contributions. This work was supported by the U.S. Department of Energy and National Science Foundation, the Italian Istituto Nazionale di Fisica Nucleare, the Ministry of Education, Science and Culture of Japan, the Natural Sciences and Engineering Research Council of Canada, the National Science Council of the Republic of China, and the A. P. Sloan Foundation.

*Now at Carnegie Mellon University, Pittsburgh, Pennsylvania 15213.

[1] N. Cabibbo, Phys. Rev. Lett. **10**, 531 (1963); M. Kobayashi and T. Maskawa, Prog. Theor. Phys. **49**, 652 (1973).
[2] Particle Data Group, R. M. Barnett *et al.,* Phys. Rev. D **54**, 1 (1996). The CKM matrix elements quoted in this edition of the Review of Particle Properties do not make use of CDF results on $|V_{tb}|$.
[3] F. Abe *et al.,* Nucl. Instrum. Methods Phys. Res., Sect. A **271**, 387 (1988).
[4] D. Amidei *et al.,* Nucl. Instrum. Methods Phys. Res., Sect. A **350**, 73 (1994).
[5] P. Azzi *et al.,* Nucl. Instrum. Methods Phys. Res., Sect. A **360**, 137 (1995).
[6] The transverse momentum, P_T, is defined as the projection of the momentum onto the plane transverse to the beam axis.
[7] The pseudorapidity, η, is defined as $\eta = -\ln[\tan(\theta/2)]$, where θ is the polar angle with respect to the proton beam direction (z axis).
[8] F. Abe *et al.,* Phys. Rev. D **50**, 2966 (1994).
[9] F. Abe *et al.,* Phys. Rev. Lett. **74**, 2626 (1995).
[10] S. Abachi *et al.,* Phys. Rev. Lett. **74**, 2632 (1995).
[11] The missing transverse energy, $\not\!\!E_T$, is defined as the negative of the vector sum of transverse energy in all calorimeters towers with $|\eta| < 3.6$.
[12] The transverse energy, E_T, is defined as the projection of the energy onto the plane transverse to the beam axis.
[13] T. Affolder *et al.* Report No. FNAL-PUB-01/007-E, 2001 [Phys. Rev. D (to be published)].
[14] F. Abe *et al.,* Phys. Rev. Lett. **80**, 2767 (1998).
[15] T. Sjöstrand, Comput. Phys. Commun. **82**, 74 (1994).
[16] F. Abe *et al.,* Phys. Rev. Lett. **80**, 2773 (1998).
[17] F. Abe *et al.,* Phys. Rev. Lett. **80**, 2779 (1998).
[18] F. Abe *et al.,* Phys. Rev. Lett. **80**, 2525 (1998).
[19] F. Abe *et al.,* Phys. Rev. Lett. **79**, 357 (1997).